JOURNAL OF MAGNETIC RESONANCE 76, 149–154 (1988)

Phase-Incremented Multiple-Quantum NMR Experiments*

D. N. SHYKIND, J. BAUM,† S.-B. LIU,‡ AND A. PINES

Department of Chemistry, University of California, Berkeley, and Materials and Chemical Sciences Division, Lawrence Berkeley Laboratory, Berkeley, California 94720

AND

A. N. GARROWAY

Code 6120, Naval Research Laboratory, Washington, D.C. 20375

Received July 2, 1987

Time-resolved multiple-quantum (MQ) NMR is a useful tool for determining the spatial distribution of atoms in materials lacking long-range order. Recently, proton MQ NMR using time proportional phase incrementation (TPPI) (*1–3*) has been applied to NMR imaging of solids (*4*), the study of hydrogen distribution in solids (*5, 6*), and hydrogenated amorphous silicon (*7*). By use of a modification of the conventional MQ experiment suggested by Emid (*8*), it is possible to improve the sensitivity and efficiency for clustering studies. Related ideas have appeared in the context of NMR imaging (*9, 10*). We explain herein experimental details of this modification, called "phase-incremented MQ NMR," and show results of spin clustering studies in solid and liquid crystalline samples.

To appreciate how phase-incremented MQ NMR works (*8*), it is useful to review the time-domain MQ experiment described schematically in Fig. 1a. As usual, the sequence can be partitioned into four distinct periods; namely the preparation (τ), evolution (t_1), mixing (τ'), and detection (t_2) periods. The pulse sequence applied during the preparation period determines the multiple-quantum excitation. For example, the eight-pulse sequence shown in Fig. 1b generates the following average dipolar Hamiltonian (*13*):

$$\bar{\mathscr{H}}_D = \frac{1}{3}(\mathscr{H}_{yy} - \mathscr{H}_{xx})$$

$$= -\frac{1}{2}\sum_{j<k} D_{jk}(I_{j+}I_{k+} + I_{j-}I_{k-}), \qquad [1]$$

where $I_{j\pm} = I_{jx} \pm iI_{jy}$, D_{jk} is the homonuclear dipolar coupling, and $\mathscr{H}_{zz}$ is the usual

* The U.S. Government's right to retain a nonexclusive royalty-free license in and to the copyright covering this paper, for governmental purposes, is acknowledged.

† Present address: Inorganic Chemistry Laboratory, University of Oxford, South Parks Road, Oxford, England OX1 3QR.

‡ Present address: Institute of Atomic and Molecular Sciences, Academia Sinica, P.O. Box 23-166, Taipei, Taiwan, R.O.C.

0022-2364/88 $3.00

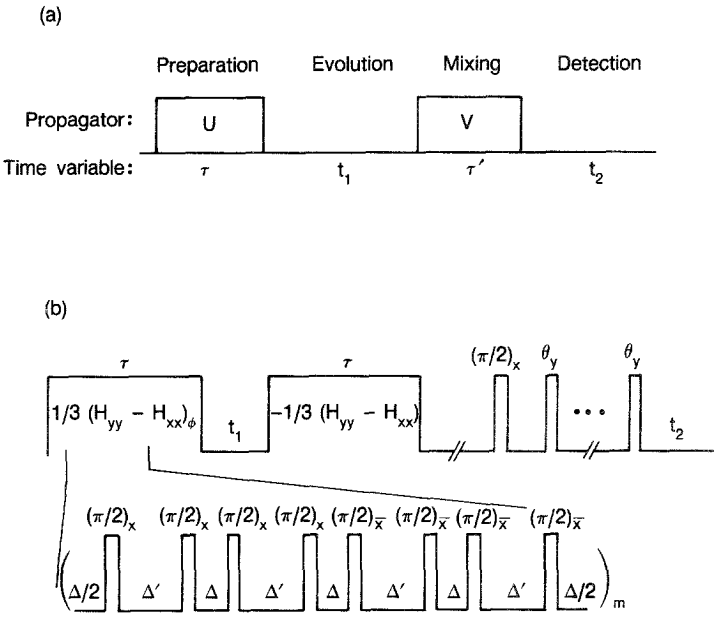

FIG. 1. (a) A schematic of time-domain MQ experiment. (b) Time-reversal pulse sequence for solid-state MQ NMR. The preparation and mixing propagators are generated by m cycles of eight $\pi/2$ pulses with width t_p and delays Δ and $\Delta' = 2\Delta + t_p$. Time reversal requires that $U = V^+$. This is implemented by changing the x, $\bar{x}$ pulses in the preparation period to y, $\bar{y}$ pulses in the mixing period. The z component of the magnetization which remains following the mixing period is sampled during t_2 by any number of methods, e.g., a single pulse or, as shown here, via a pulsed spin-lock sequence (*11, 12*). Typical spin-lock pulse width (θ_y) is about $\pi/4$.

high-field dipolar Hamiltonian, quantized along z. The above Hamiltonian contains only double-quantum operators and hence excites only even order MQ coherences. During the evolution period, the MQ coherences evolve under the influence of the unaveraged internal Hamiltonian $\mathscr{H}_{zz}$ for a time t_1. In order to separate different MQ orders, the method of TPPI is used: the overall phase of the preparation pulses is incremented in proportion to t_1 according to the relation $\Delta\phi = \Delta\omega' \Delta t_1$. This phase shift with its associated time increment is equivalent to a resonance offset $\Delta\omega'$ acting during the evolution period.

During the mixing period, the MQ coherences are converted to observable Zeeman magnetization. In solids, it is helpful to use a time-reversed (*14*) mixing period to ensure that individual coherences within a MQ order can be all generated with the same phase at $\phi(t_1) = 0$. This is obtained by requiring that the propagator for the preparation period is the Hermitian conjugate of the mixing period propagator, i.e., $U = V^+$ (*4*). Experimentally, this corresponds to changing the phases of all the pulses in the preparation period by 90° with respect to the mixing pulses.

Immediately after the mixing period ($\tau = \tau'$, $t_2 = 0$) the time-domain signal can be written (*4, 5*) as

$$S(\tau, t_1) = \sum_n \sum_{j,k} |\Phi_{jk}(\tau)|^2 \exp[in\phi(t_1)] \exp(-i\omega_{jk} t_1) \qquad [2a]$$

$$= \sum_n \sum_{j,k} |\Phi_{jk}(\tau)|^2 \exp(in\Delta\omega' t_1) \exp(-i\omega_{jk} t_1). \quad [2b]$$

Here, $\Phi_{jk}(\tau) = \langle j|U^+ I_z U|k\rangle = \langle k|V I_z V^+|j\rangle$ are elements of the reduced density matrix, and $\omega_{jk} = \omega_j - \omega_k$ is defined as the MQ transition frequency between states j and k. After Fourier transformation with respect to t_1, the signal of the MQ coherence between states j and k is therefore characterized by an amplitude $|\Phi_{jk}(\tau)|^2$, an order-dependent offset term $n\Delta\omega'$, and a transition frequency ω_{jk}. For a complex spin system, there will be a range of values ω_{jk} contributing to a particular MQ coherence; this spread leads to line broadening in the t_1 domain, as the contributions are summed up as shown in Eq. [2]. Hence, under TPPI, the nth coherence will have a MQ linewidth $\omega_L(n)$, due to variations in the local dipolar field. This broadening of the MQ coherence under TPPI also requires that the apparent resonance offset frequency $\Delta\omega'$ be selected to overwhelm the MQ linewidth $\omega_L(n)$. A typical time-domain proton MQ signal generated by the TPPI method is shown in Fig. 2a for hexamethylbenzene. Fourier transformation of Eq. [2b] with respect to t_1 yields the MQ spectrum shown in Fig. 2c. The spectral width (in frequency units) of the MQ spectrum is determined by the inverse of the t_1 increment, and the number of orders detected, $\pm n_{max}$, is governed only by the phase increment $\Delta\phi = \pi/n_{max}$.

The phase-incremented MQ experiment proceeds just as described above, but with the constraint that the evolution period is held fixed, while the phases of the preparation pulses are incremented pointwise by $\Delta\phi$. In other words, the evolution period t_1 is no longer a time variable in Eq. [2a] thus "decoupling" the MQ linebroadening, in analogy to NMR imaging techniques which use a fixed evolution period (*9, 10*). Fourier transformation of Eq. [2a] with respect to ϕ will therefore give rise to a series of δ-function spikes corresponding to the multiple-quantum order n. Figure 2b is the time-domain MQ signal of hexamethylbenzene generated by such a method, and its Fourier spectrum is shown in Fig. 2d.

In MQ clustering experiments, the important information is contained in the integrated intensities of the MQ orders, rather than in the different frequencies occurring within each order. Hence, the spectrum (Fig. 2b) obtained by the phase-incremented method has a higher signal-to-noise ratio and is also more convenient in terms of data analysis. Second, for phase-incremented MQ experiments, the signal is strictly periodic with period 2π (cf. Fig. 2b). Hence, the number of "time-domain" points required in the phase-incremented scheme is considerably less than that of TPPI method. To illustrate these two points, the spectrum in Fig. 2c is a result of an overnight experiment using TPPI and signal averaging. The spectrum in Fig. 2d was obtained under comparable experimental conditions in less than five minutes. Instrumental stability is crucial for success in these experiments. Instabilities in the phase shifter (*15*) used to generate the preparation period phase shifts or phase transients (*16*) in the multiple-pulse trains used for the preparation and mixing periods can produce intensity distortions in the MQ spectrum. Such distortions preclude accurate cluster size measurements.

As a demonstration, the results of phase-incremented MQ NMR studies of clustering in solids are shown in Figs. 3a and 3b for different spatial distributions that were determined previously (*6*). In brief, the intensities $I(n)$ across the MQ orders can be described by a Gaussian distribution (*6, 17*):

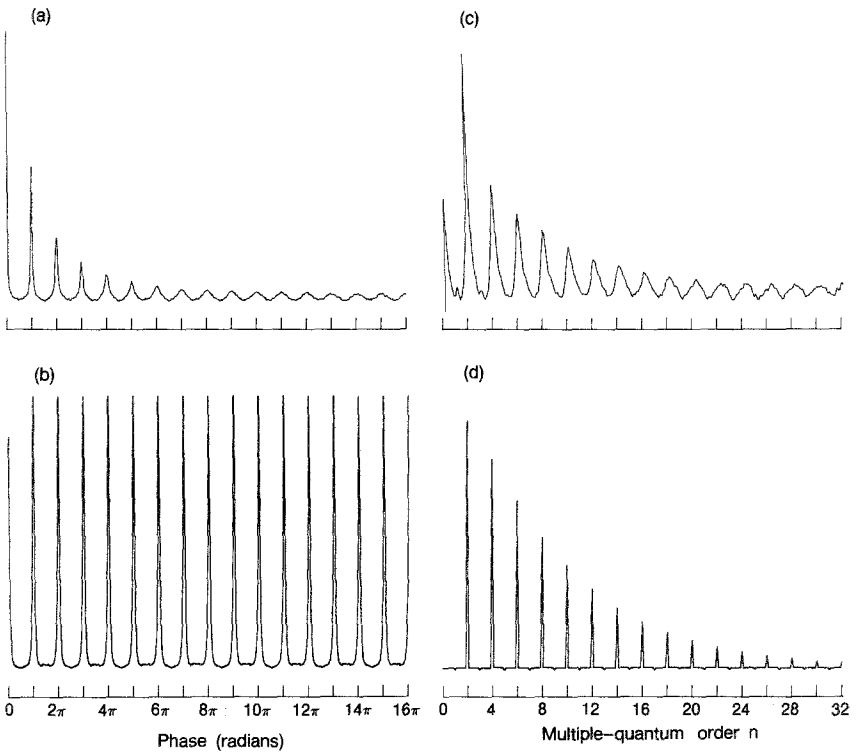

FIG. 2. Multiple-quantum NMR signals of hexamethylbenzene. (a) Time-domain MQ interferogram using the TPPI method and the pulse sequence shown in Fig. 1b. The experimental parameters used are $\Delta = 2.5$ μs, $t_p = 3$ μs, $\Delta' = 8$ μs, unit cycle time $\tau_c = 66$ μs, number of cycles $m = \tau/\tau_c = 8$, $\Delta t_1 = 100$ μs, and $\Delta\phi = \pi/32$ radians. The spectrum was obtained on a 180 MHz spectrometer. (b) Similar to (a) but using the phase-incremented method described in the text. Here, $\Delta = 2$ μs, $t_p = 4$ μs, $\Delta' = 8$ μs, $\tau_c = 72$ μs, $m = 8$, fixed $t_1 = 2$ μs, and $\Delta\phi = \pi/128$. A 100 MHz spectrometer at NRL was used. Notice that, for this even-quantum excitation, the signal is periodic over π radians. The signal is strictly periodic over a full 2π radians, and the data over the first 2π have been translated to fill 16π radians, to facilitate comparison with (a). (c) A Fourier transform of (a) with respect to t_1 yields a spectrum with broad lines, each appearing at even MQ orders. The intensity of the zero-quantum line is arbitrary. (d) Fourier transform of (b) with respect to phase ϕ in the phase-incremented MQ experiment. The MQ lines are now infinitely narrow, as expected; the apparent width arises from the plotter connecting the data points.

$$I(n) = A \exp(-n^2/N), \qquad \text{for } N \geq 6. \qquad [3]$$

Here, A is the normalization constant and N is the apparent cluster size which develops over the time τ. Liquid crystals in their nematic phase are the simplest example of isolated clusters in which MQ intensities can be described (*6*) by Eq. [3]. A plot of the effective cluster size as a function of preparation time τ in a nematic liquid crystal ^{15}K (*p*-cyano-*p*-*n*-pentylbiphenyl; $C_{18}H_{19}N$) is shown in Fig. 3a. The plateau at about $N = 20$ in Fig. 3a is consistent with the fact that rapid translational diffusion averages the intermolecular dipole coupling to zero, allowing only the 19 ^{1}H spins *within* the molecule to correlate with one another. On the other hand, for a continuous distribution of spins, the effective cluster size should increase monotonically with increasing preparation time τ. This is readily seen for solid hexamethylbenzene as displayed in Fig. 3b, showing correlations among over 200 spins.

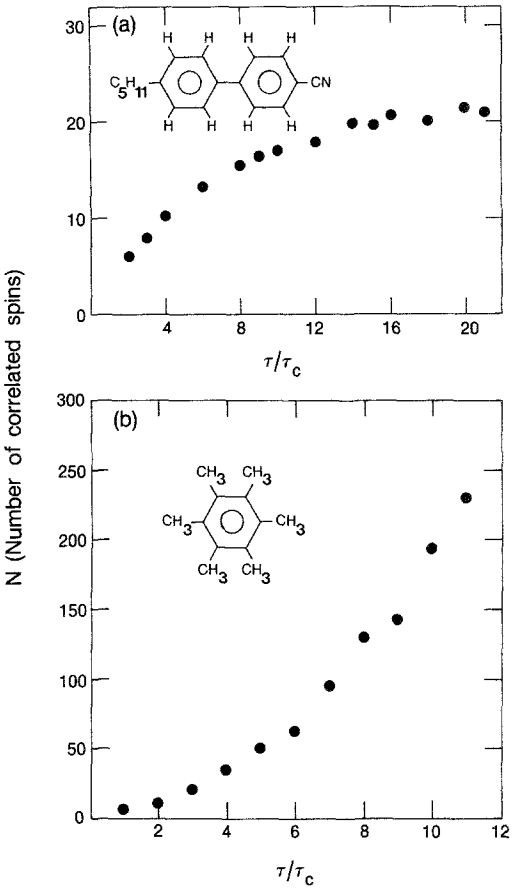

FIG. 3. Phase-incremented proton MQ NMR results. The number of correlated spins (N) is plotted against the number of cycles τ/τ_c. (a) The results for nematic ^{15}K liquid crystal (containing 19 hydrogens). The basic cycle time τ_c was 62 μs in these experiments; the plateau at $N \approx 20$ reflects the fact that in the nematic phase of a liquid crystal, the spin clusters are truly isolated. (b) The results of phase-incremented MQ NMR on a continuous spin system; proton distribution in bulk hexamethylbenzene powder. The effective cluster size increases monotonically.

It is important to note that eliminating the linewidth information in a MQ NMR experiment is not always desirable. For example, in hydrogenated amorphous silicon (*7*) the NMR absorption line can be deconvoluted into two components. Information can perhaps be obtained from linewidths and lineshapes in the other MQ experiments as well, necessitating the use of a conventional TPPI experiment. However, when integrated MQ intensities are required, rather than lineshape information, then phase incrementation provides a sensitive and time-efficient version of multiple-quantum NMR.

ACKNOWLEDGMENTS

The work at Berkeley was supported by the Director, Office of Energy Research, Office of Basic Energy Sciences, Materials Science Division of the U.S. Department of Energy, under Contract DE-AC03-76SF00098.

J.B. held a University of California Presidents Fellowship. We gratefully thank Dr. D. Suter for helpful discussions and for providing a data analysis program.

REFERENCES

1. G. DROBNY, A. PINES, S. SINTON, D. P. WEITEKAMP, AND D. WEMMER, *Faraday Symp. Chem. Soc.* **13,** 49 (1979).
2. G. BODENHAUSEN, R. L. VOLD, AND R. R. VOLD, *J. Magn. Reson.* **37,** 93 (1980).
3. A. PINES, *in* "Proceedings of the Fermi School on the Physics of NMR in Biology and Medicine" (B. Maraviglia, Ed.), in press.
4. A. N. GARROWAY, J. BAUM, M. G. MUNOWITZ, AND A. PINES, *J. Magn. Reson.* **60,** 337 (1984).
5. J. BAUM, M. MUNOWITZ, A. N. GARROWAY, AND A. PINES, *J. Chem. Phys.* **83,** 2015 (1985).
6. J. BAUM AND A. PINES, *J. Am. Chem. Soc.* **108,** 7447 (1986).
7. J. BAUM, K. K. GLEASON, A. PINES, A. N. GARROWAY, AND J. REIMER, *Phys. Rev. Lett.* **56,** 1377 (1986).
8. S. EMID, *Physica B* **128,** 79 (1985).
9. W. A. EDELSTEIN, J. M. S. HUTCHISON, G. JOHNSON, AND T. REDPATH, *Phys. Med. Biol.* **25,** 751 (1980).
10. S. EMID AND J. H. N. CREYGHTON, *Physica B* **128,** 81 (1985).
11. W.-K. RHIM, D. P. BURUM, AND D. D. ELLEMAN, *Phys. Rev. Lett.* **37,** 1764 (1976).
12. Y. S. YEN, Ph.D. thesis, University of California, Berkeley, 1982.
13. W. S. WARREN, D. P. WEITEKAMP, AND A. PINES, *J. Chem. Phys.* **73,** 2084 (1980).
14. W.-K. RHIM, A. PINES, AND J. S. WAUGH, *Phys. Rev. B* **3,** 684 (1971).
15. A. N. GARROWAY, *J. Magn. Reson.* **63,** 504 (1985).
16. M. MEHRING AND J. S. WAUGH, *Rev. Sci. Instrum.* **43,** 649 (1972).
17. J. B. MURDOCH, W. S. WARREN, D. P. WEITEKAMP, AND A. PINES, *J. Magn. Reson.* **60,** 205 (1984).